

Expansion of the Substrate Specificity of Porcine Kidney D-Amino Acid Oxidase for *S*-Stereoselective Oxidation of 4-Cl-Benzhydrylamine

Kazuyuki Yasukawa,^[a, b] Fumihito Motojima,^[a, b] Atsushi Ono,^[a] and Yasuhisa Asano^{*[a, b]}

Discovery and development of enzymes for the synthesis of chiral amines have been a hot topic for basic and applied aspects of biocatalysts. Based on our X-ray crystallographic analyses of porcine kidney D-amino acid oxidase (pkDAO) and its variants, we rationally designed a new variant that catalyzed the oxidation of (*S*)-4-Cl-benzhydrylamine (CBHA) from pkDAO and obtained it by functional high-throughput screening with colorimetric assay. The variant I230A/R283G was constructed from the variant R283G which had completely lost the activity for D-amino acids, further gaining new activity toward (*S*)-chiral amines with the bulky substituents. The variant enzyme (I230A/

R283G) was characterized to have a catalytic efficiency of 1.85 s^{-1} for (*S*)-CBHA, while that for (*R*)-1-phenylethylamine was diminished 10-fold as compared with the Y228L/R283G variant. The variant was efficiently used for the synthesis of (*R*)-CBHA in 96% *ee* from racemic CBHA by the deracemization reaction in the presence of reducing agent such as NaBH_4 in water. Furthermore, X-ray crystallographic analysis of the new variant complexed with (*S*)-CBHA, together with modelling study clearly showed the basis of understanding the structure-activity relationship of pkDAO.

Introduction

Extensive efforts have been made on the discovery and development of efficient biocatalysts used for the chiral amine synthesis of building blocks for pharmaceuticals. Lipases and transaminases have been well studied and used for the practical kinetic resolution of amines to produce chiral amines; however, the yields of these methods are limited because the reactions are kinetic resolution or equilibrium reactions, respectively.^[1a,b] To overcome the limitation inherent with the use of lipase B from *Candida antarctica*, Reetz and Schimossek in 1996 first introduced the dynamic kinetic resolution reaction with a racemization of the by-product (*S*)-1-phenylethylamine (**1a**) in the presence of palladium, thereby improving the final yield of (*R*)-**1a** to the theoretical 100%.^[2] Koszelewski et al. reported the synthesis of optically active mexiletine by the deracemization procedure using stereoselective transaminases, although *R*- and *S*-selective enzymes have to be stereocomplementary.^[3]

Recently, new biocatalysts for chiral amine synthesis were developed by directed evolution.^[4a,b] Bommarius et al. have presented the production of (*R*)-amines from corresponding ketones using the developed amine dehydrogenase from already known amino acid dehydrogenases with an NADH cofactor regeneration system, but a short life-time of the enzyme was observed when highly hydrophobic ketones were used as the substrates in an aqueous-organic solvent system.^[5a,b] Turner et al. reported a deracemization reaction that uses an engineered *S*-stereoselective monoamine oxidase from *Aspergillus niger* in the presence of a reductant.^[6a,b,c] The oxidase-catalyzed deracemization method has merit in that it does not need to be conjugated with other enzymes compared to the systems that use amine transaminase or amine dehydrogenase.

R-stereoselective amine oxidases (AOD) that are applicable to the deracemization of amines are a relatively recent discovery. Engineered 6-hydroxy-D-nicotine oxidase (E350L/E352D) catalyzing (*R*)-nicotine oxidation with moderate activity was reported.^[7] We have reported that a variant porcine kidney D-amino acid oxidase (pkDAO) (Y228L/R283G) catalyzed the synthesis of (*S*)-**1a** by deracemization. The variant completely lost activity for D-amino acids, although the starting pkDAO has a rather wide substrate specificity for D-amino acids.^[8a,b] We solved the structure of the variant pkDAO (Y228L/R283G) in complex with FAD and (*R*)-**1a** to a resolution of 1.88 Å by X-ray crystallography (PDB: 3WGT). We designed the enzyme to lose activity for D-amino acids by removing the residues that recognize the carboxylic acid of the substrate; made a rational explanation for the new high activities for (*R*)-**1a**; and explained how D-amino acids such as D-phenylalanine (**3**), D-methionine, and D-proline were no longer the substrate. This variant best catalyzed the oxidation of (*R*)-**1a** as a substrate, while a bulky substrate such as benzhydrylamine (**2a**) was not compatible.

[a] Dr. K. Yasukawa, Dr. F. Motojima, M. Sci. A. Ono, Prof. Dr. Y. Asano
Biotechnology Research Center and Department of Biotechnology
Toyama Prefectural University
5180 Kurokawa, Imizu, Toyama 939-0398, Japan
E-mail: asano@pu-toyama.ac.jp

[b] Dr. K. Yasukawa, Dr. F. Motojima, Prof. Dr. Y. Asano
Asano Active Enzyme Molecule Project
Toyama Prefectural University
5180 Kurokawa, Imizu, Toyama 939-0398, Japan

Supporting information for this article is available on the WWW under <https://doi.org/10.1002/cctc.201800614>

©2018 The Authors. Published by Wiley-VCH Verlag GmbH & Co. KGaA.
This is an open access article under the terms of the Creative Commons Attribution Non-Commercial NoDerivs License, which permits use and distribution in any medium, provided the original work is properly cited, the use is non-commercial and no modifications or adaptations are made.

The aim of this study is to obtain variants of pkDAO that act on benzhydrylamine compounds and are applicable to the deracemization reaction to produce (*R*)-4-chlorobenzhydrylamine (**2c**) and 4-substituted benzhydrylamine compound, which are useful chiral building blocks for pharmaceuticals. Our strategy is based on our experimental data from the structure-activity relationship among the functional amino acid residues in the active site of the parent and variant Y228L/R283G together with our systematic and effective screening system.

Results and Discussion

Screening for Benzhydrylamine Oxidase

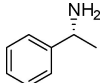
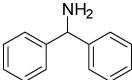
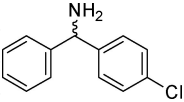
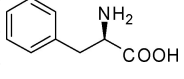
Recently, we described a variant (Y228L/F242I/R283G) catalyzing the oxidation of 1-(2-naphthyl)ethylamine ($k_{\text{cat}}/K_m = 0.83 \text{ s}^{-1} \text{ mM}^{-1}$) and showed a possibility of broadening the substrate specificity based on the computational analysis of its crystal structure.^[9] Based on the crystal structure of variant Y228L/R283G, we speculated that 4-Cl-phenyl ring of (*S*)-**2c** would be directed toward the hydrophobic cavity formed by Leu51, Ile215, and Ile230, and that the cavity at the active site would play a key role in accommodating the bulky substrate.^[10] It would be possible to discriminate between the 4-Cl-phenyl group and the non-substituted phenyl group in **2c** if we carefully choose the residues of the cavity. Therefore, the residues Leu51, Ile215, and Ile230 in the active site of pkDAO were chosen as targets for mutation to improve the catalytic properties. Variants R283G and Y228L/R283G were chosen as parents for the saturation mutagenesis of Leu51, Ile215, and Ile230. Then, high-throughput screening by a colorimetric assay using 96 well microtiter plates was used to determine the oxidation activity toward **2a** and (*RS*)-**2c** by the formation of

red pigment. Four variants of the mutant, I230A/R283G, I230C/R283G, I230F/R283G, and Y228L/I230C/R283G, were obtained as positive clones from the screening library of saturation mutagenesis at Ile230. All of these variants catalyzed *S*-stereoselective oxidizing activity toward **2c**, while all of the variants obtained by the saturation mutagenesis at Leu51 and Ile215 did not show any enzyme activity toward these substrates. A unique variant, I230V/R283G, was obtained that also catalyzed the oxidation of **2a**, but not **2c**. Our result showed that Ile230 was a very important residue to accommodate substrates such as benzhydrylamine. On the other hand, Ile215 in pkDAO, which corresponds to Met213 in DAO from *Rhodotorula gracilis* as proposed by Pollegioni et al.,^[10] plays an important role of recognizing the side chain of the substrate D-amino acid. They actually reported that the variant M213G efficiently catalyzed the oxidation of unnatural bulky (*R*)-amino acids such as naphthyl derivatives.^[10b,c] Therefore the mutation of Ile215 in the variant I230A is expected to broaden the substrate specificity to accommodate the bulky group of C_β such as α-(2-naphthyl)benzylamine.

Kinetic Parameter and Substrate Specificity

All the engineered variant enzymes were purified as described in the experimental section. A variant with three point mutations, Y228L/I230C/R283G, seems to lose its enzymatic activity. This is probably because of the loss of the FAD cofactor from the enzyme because the yellow color of the enzyme disappeared during the purification process. The kinetic parameters of the variant enzymes, I230A/R283G, I230C/R283G, and I230F/R283G, were determined to evaluate the effects of the mutations (Table 1). Compared with the variant R283G, variants I230A/R283G, I230C/R283G, and I230F/R283G showed lower

Table 1. Kinetic parameter of wild-type and variants pkDAO.

Substrate	Parameter	Wild-type	Y228L	R283G	Y228L/R283G	I230A/R283G	I230C/R283G	I230F/R283G
 (R)-1a	K_m [mM]	n.d. ^[a]	n.d.	6.98 ± 0.67	7.95 ± 0.78	7.28 ± 0.90	6.90 ± 1.11	6.25 ± 0.89
	k_{cat} [s^{-1}]	n.d.	n.d.	1.46 ± 0.08	9.93 ± 0.88	0.349 ± 0.013	0.111 ± 0.014	0.0474 ± 0.0059
	k_{cat}/K_m [$\text{s}^{-1} \text{ mM}^{-1}$]	n.d.	n.d.	0.211	1.26	0.0482	0.0161	0.00777
 2a	K_m [mM]	n.d.	n.d.	n.d.	n.d.	5.23 ± 0.65	2.40 ± 0.30	2.63 ± 0.43
	k_{cat} [s^{-1}]	n.d.	n.d.	n.d.	n.d.	3.30 ± 0.49	3.42 ± 0.30	0.366 ± 0.036
	k_{cat}/K_m [$\text{s}^{-1} \text{ mM}^{-1}$]	n.d.	n.d.	n.d.	n.d.	0.629	1.45	0.141
 (RS)-2c	K_m [mM]	n.d.	n.d.	n.d.	n.d.	2.94 ± 0.23	2.96 ± 0.23	3.73 ± 0.34
	k_{cat} [s^{-1}]	n.d.	n.d.	n.d.	n.d.	6.01 ± 0.10	5.48 ± 0.46	4.33 ± 0.98
	k_{cat}/K_m [$\text{s}^{-1} \text{ mM}^{-1}$]	n.d.	n.d.	n.d.	n.d.	2.05	1.85	1.15
 (R)-3	K_m [mM]	5.01 ± 0.27	8.41 ± 2.24	n.d.	n.d.	n.d.	n.d.	n.d.
	k_{cat} [s^{-1}]	5.19 ± 0.09	1.72 ± 0.01	n.d.	n.d.	n.d.	n.d.	n.d.
	k_{cat}/K_m [$\text{s}^{-1} \text{ mM}^{-1}$]	1.04	0.215	n.d.	n.d.	n.d.	n.d.	n.d.

[a] n.d.: not detected.

k_{cat}/K_m values toward (*R*)-**1a**. In contrast, the newly evolved variants were able to catalyze the oxidation of (*S*)-**2c**. The variant I230A/R283G showed the highest k_{cat}/K_m value toward (*S*)-**2c** amongst the variants (Table 2). Therefore, variant I230A/

ring of **2c** weakly interacted with Tyr228. The position of the amine group and α -carbon of (*S*)-**2c** are similar to those of (*R*)-**1a** in Y228L/R283G suggesting that the oxidation mechanism (a hydride transfer) is not changed (Figure 1).^[11a,b]

Table 2. Substrate specificity of variant pkDAO Y228L/R283G and I230A/R283G. ^[a]						
Substrate	Variants pkDAO		Y228L/R283G ^[b]		I230A/R283G ^[b]	
	R ¹	R ²	Y228L/R283G ^[b]	I230A/R283G ^[b]	Y228L/R283G ^[b]	I230A/R283G ^[b]
(<i>R</i>)- 1a	C ₆ H ₅	CH ₃	100	2.4		
(<i>S</i>)- 1a	C ₆ H ₅	CH ₃	< 0.1	< 0.1		
(<i>R</i>)- 1b	4-F-C ₆ H ₄	CH ₃	33.6	0.9		
(<i>S</i>)- 1b	4-F-C ₆ H ₄	CH ₃	< 0.1	< 0.1		
(<i>R</i>)- 1c	4-Cl-C ₆ H ₄	CH ₃	5.0	< 0.1		
(<i>S</i>)- 1c	4-Cl-C ₆ H ₄	CH ₃	< 0.1	< 0.1		
2a ^[c]	C ₆ H ₅	C ₆ H ₅	n.d. ^[e]	10.9		
(<i>RS</i>)- 2b ^[c]	4-F-C ₆ H ₄	C ₆ H ₅	n.d.	46.5		
(<i>RS</i>)- 2c ^[c]	4-Cl-C ₆ H ₄	C ₆ H ₅	n.d.	45.2		
(<i>R</i>)- 2c ^[c]	4-Cl-C ₆ H ₄	C ₆ H ₅	n.d.	< 0.1		
(<i>S</i>)- 2c ^[c]	4-Cl-C ₆ H ₄	C ₆ H ₅	n.d.	84.8		
(<i>RS</i>)- 2d ^[d]	4-Br-C ₆ H ₄	C ₆ H ₅	n.d.	8.1		
(<i>R</i>)- 3	C ₆ H ₅ CH ₂	CO ₂ H	n.d.	n.d.		

[a] The reaction mixture contained the substrate, 100 mM KPB (pH 8.0), 2 mM phenol, 1.5 mM 4-aminoantipyrine, 2 U horseradish peroxidase, 10% DMSO and the amount of enzyme; unless otherwise stated, the substrates were used at a final concentration of 10 mM. [b] The activity of variant Y228L/R283G toward (*R*)-**1a** was taken as 100% (18.3 U/mg). [c] Substrates used at a final concentration of 5 mM. [d] Substrates used at a final concentration of 1 mM. [e] n.d.: not detected.

R283G was selected for further investigation. The stereoselectivity shown by variant I230A/R283G for **2c** was confirmed by using (*S*)- and (*R*)-**2c**. The enzyme acted on (*R*)-**2c** with only negligible activity. The K_m values of variant I230A/R283G for (*S*)- and (*R*)-**2c** were 2.80 mM and 1.99 mM, respectively and their k_{cat} values were calculated to be 7.30 s⁻¹ and 0.006 s⁻¹, respectively (Table S1). From these results, the enantiomeric ratio (*E*-value) for the *S*-enantiomer of **2c** was calculated by the following Eq. (1).

$$E\text{-value} = [k_{\text{cat}}/K_m](S\text{-enantiomer})/[k_{\text{cat}}/K_m](R\text{-enantiomer}) \quad (1)$$

The *E*-value for (*S*)-**2c** was calculated to be higher than 1000, which is enough to be utilized in the kinetic resolution of (*RS*)-**2c**. To understand the manner of chiral discrimination toward **2c**, the variant I230A/R283G was subjected to X-ray crystallographic analysis.

The crystal structure of variant I230A/R283G complexed with (*S*)-**2c** was determined at 3.20 Å resolution (PDB: 5WWV). In five out of eight molecules, the electron density corresponding to (*S*)-**2c** was observed, even though the similar K_m values for (*S*)- and (*R*)-**2c** indicate that the affinities of I230A/R283G are similar. This mutation would have made additional space to accommodate the 4-Cl-phenyl ring of **2c**, and the 4-Cl-phenyl

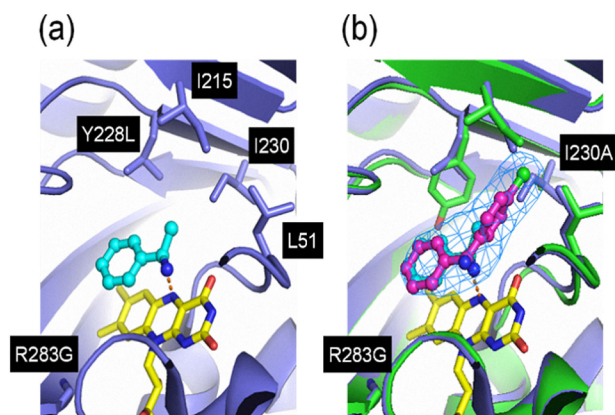


Figure 1. The ligand binding in the active site of pkDAO variants. (a) The cartoon model of pkDAO (Y228L/R283G)-(R)-**1a** complex. (*R*)-**1a** is shown as ball-and-stick model colored cyan. FAD is colored in yellow. The residues mutated for the screening of the variants oxidizing (*S*)-**2c** are labeled and shown as stick model. (b) The superposition of pkDAO (Y228L/R283G)-(R)-**1a** complex (blue) and pkDAO (I230A/R283G)-(S)-**2c** complex (green). (*S*)-**2c** is shown as ball-and-stick model colored magenta. The α_A -weighted F_o-F_c omit map ($> 4.0\sigma$) of (*S*)-**2c** is shown in blue mesh. The mutated residues are labeled. The distance of α -carbon of (*R*)-**1a** and (*S*)-**2c** to N5 atom of isoalloxazine ring are shown as orange dotted lines (3.15 and 3.48 Å, respectively).

However, we could not explain why the variant I230F/R283G also showed oxidation activity toward (*S*)-**2c**, because it was speculated that substituted phenylalanine would hinder access of the 4-Cl-phenyl ring of (*S*)-**2c** to the newly formed hydrophobic cavity. To explain this question, we constructed a three-dimensional model of I230F/R283G using MOE based on the crystal structure of variant I230A/R283G (Figure S3). Interestingly, a shift outward in the active site of the benzene ring of Phe230 toward Ile138 and the C δ 1 atom of Ile138 was observed. As a result, the enough space to accept the chloride moiety of (*S*)-**2c** was created (Figure S3).

As a result of the studies on the substrate specificity, I230A/R283G showed activities toward (*R*)-**1a** and (*R*)-**1b**, while (*R*)-**1c**, (*S*)-**1a**, (*S*)-**1b**, and (*S*)-**1c** were not substrates and had negligible activities (Table 2). These results suggest that the interaction of phenyl ring of **2c** with Tyr224 as well as the isoalloxazine ring of FAD by π - π stacking and also Phe242 by the T-shaped stacking, which play a more important role in substrate recognition than the hydrophobic cavity formed by Leu51, Ile215 and Ile230.

Docking simulation of **1b** with the active site of variant I230A/R283G supported this suggestion. (*R*)-**1b** preferred to bind in the active site in a position similar to that of (*R*)-**1a** in the crystal structure of Y228L/R283G, but the corresponding *S*-enantiomer could not bind to anywhere in the enzyme.

Deracemization Reaction using Variant pkDAO (I230A/R283G)

Optically active products have been obtained at the theoretical yield of 100% in the oxidase-catalyzed deracemization reaction of amines with the use of chemical reductants such as NaBH_4 . Furthermore, this process has merit since a complicated separation of the remaining substrate and the product are generally not necessary because the structure of the starting substrate and the product is the same. The optimization of the deracemization reaction such as the effects of buffers, pH, and reductants show that the best condition is as follows: the reaction mixture (total volume 1 ml) contained 100 mM glycine-NaOH (pH 9.0), 5 mM (*RS*)-**2c**, 100 mM NaBH_4 , and 0.4 U of the purified enzyme in an aqueous medium shaken at 1.7×10^3 rpm at 30 °C. In the optimized deracemization condition, (*R*)-**2c** was obtained in 98.0% e.e. within 1 h because (*S*)-**2c** was converted to the corresponding imine-**2c** by pkDAO I230A/R283G, and then the imine was immediately reduced to (*RS*)-**2c** by NaBH_4 (Figure 2). In this reaction, undesirable by-products such as

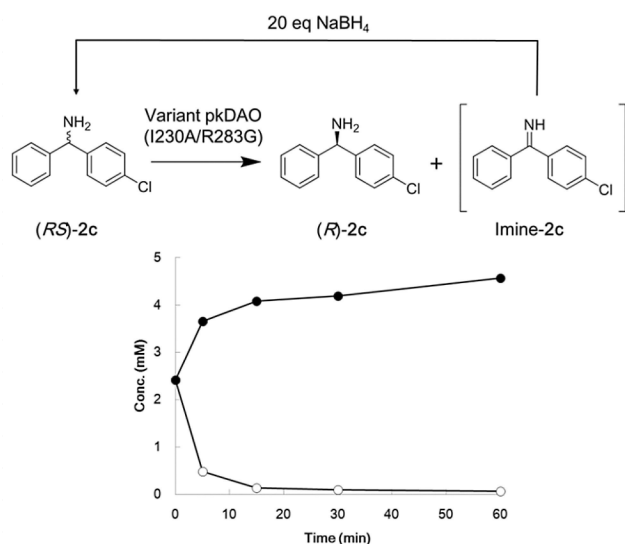


Figure 2. Time course of the deracemization of **2c** using variant I230A/R283G. The reaction mixture (1 mL) consisted of 100 mM glycine-NaOH buffer (pH 9.0), 5 mM (*RS*)-**2c**, 100 mM NaBH_4 , and 0.1 U purified enzyme, and the reaction mixture was stirred at 1.3×10^3 rpm at 30 °C. Symbol; ●: (*R*)-**2c**, ○: (*S*)-**2c**.

ketones and alcohols were not detected. Previously, Turner et al. reported the deracemization of 1 mM of **2c** with an *S*-selective monoamine oxidase variant D11C from *Aspergillus niger* for 48 h at 37 °C using $\text{NH}_3\text{-BH}_3$ as a reductant.^[6b] Compared with that study, the deracemization reaction by pkDAO I230A/R283G with the reductant NaBH_4 gave a pure (*R*)-**2c** in a short time. However, addition of too much NaBH_4 caused denaturation of the enzyme. Recently, a more eco-friendly oxidase-catalyzed deracemization method by imine reductase and an artificial transfer hydrogenase as a reductant in substitution for the chemical reductant was reported.^[12a,b] However, these non-chemical reductants have limits in the

selection of the substrate; for example, only cyclic amines, which generate stable imine under the aqueous buffer by AOD, can be used as substrates. More recently, Aleku et al. reported the synthesis of chiral secondary amine by unique deracemization method using reductive amination in combination with NADP^+ -regeneration system in the presence of $\text{NH}_3\text{-BH}_3$.^[13] On the other hand, an unstable imine formed from a straight chain primary amine, such as **1a** catalyzed by AOD, is quickly converted to the corresponding ketone by aqueous hydrolysis. A control of an unstable straight chain imine as an intermediate formed during the deracemization reaction would be a new challenge for the next generation of deracemization reactions.

A preparative scale reaction was carried out for identification of the product by the deracemization reaction using variant I230A/R283G. The reaction product was easily purified by extraction with hexane (40 mL \times 3) under alkaline conditions, and then, the hexane layer was evaporated *in vacuo*. The resulting oil residue was further dried in a desiccator. The final product (19.8 mg) was identified as (*R*)-**2c** (46.2% yield and 95.7% e.e.) from HPLC analysis, $^1\text{H-NMR}$ spectra and by examination of the optical rotation with ATAGO AP-300 polarimeter (Figure S4 and S5). Result of $^1\text{H-NMR}$ spectra in isolated product confirmed remaining H_2O and DMSO. HPLC analysis showed a small amount of the by-product alcohol in deracemization reaction eluted at 3.7 min.

Conclusions

We obtained a novel variant I230A/R283G from pkDAO by protein engineering based on our X-ray crystallographic analyses of the variant Y228L/R283G and utilized it in the synthesis of (*R*)-**2c** by the deracemization method with NaBH_4 . Determination of the three-dimensional structure of the variant I230A/R283G complexed with the substrate (*S*)-**2c** is a proof of concept of our mutagenesis strategy. DAO has been widely found in eukaryotic and prokaryotic organisms, and these enzymes showed variation in enzymatic properties such as optimum reaction condition, substrate specificity, and amino acid sequence. In the future, we should be able to design several new amine oxidases evolved from amino acid oxidases having desirable stereoselectivity for several amines to establish the next generation of green chemistry.

Experimental Section

Materials

(*R*)- α -1-phenylethylamine, (*S*)- α -1-phenylethylamine, (*R*)-4-F- α -1-phenylethylamine, (*S*)-4-F- α -1-phenylethylamine, (*R*)-4-Cl- α -1-phenylethylamine, (*S*)-4-Cl- α -1-phenylethylamine, (*RS*)-4-Cl-benzhydrylamine, and benzhydrylamine were obtained from Sigma-Aldrich (Munich, Germany). (*R*)-4-Cl-benzhydrylamine was purchased from Astatech, Inc (Bristol, PA., USA). (*S*)-4-Cl-benzhydrylamine was purchased from Combi-Blocks (San Diego, CA., USA). (*RS*)-4-F-benzhydrylamine and (*RS*)-4-Br-benzhydrylamine were synthesized

in our laboratory (supporting information). All other chemicals were commercially available.

Site-directed Mutagenesis

Saturation mutagenesis of plasmid pDAOR283G or pDAOY228L/R283G as a template was carried out with QuikChange Lightning Site-Directed Mutagenesis Kit (Stratagene, California, USA), and then it was used to transform the *E. coli* JM109. These mutants were cultivated at 37 °C for 24 hr on an LB agar plate containing 80 µg/mL ampicillin, and then single colonies were cultivated at 37 °C for 24 hr in 100 µL LB media containing 80 µg/mL ampicillin and 1 mM IPTG in a Nunc™ DeepWell™ plate. After the cultivation, cells were collected by centrifugation and suspended in 100 µL 100 mM potassium-phosphate buffer (KPB) (pH 8.0). Intact cells were suspended (10 µL) in the reaction mixture (100 µL), which consisted of 100 mM KPB (pH 8.0), 2 mM phenol, 1.5 mM 4-aminoantipyrine, 2 U horseradish peroxidase, and a substrate, such as (R)-**1a**, **2a**, or (RS)-**2c**.

DNA Sequence Analysis

Nucleotide sequencing was performed using the dideoxynucleotide chain termination method. Sequencing reactions were carried out with a BigDye® Terminator v3.1 Cycle Sequencing Kit (Applied Biosystems, Foster City, CA., USA), and the reaction mixture was applied to an ABI PRISM 310 Genetic analyzer (Applied Biosystems, Foster City, CA., USA).

Purification of wild-type pKDAO and variant pKDAOs

All enzymes were purified by the same procedure. *E. coli* cells were suspended in 5 volumes of 10 mM KPB (pH 8.0) containing 0.1% 2-mercaptoethanol and disrupted by sonication for 20 min at 180 W using Insonator 201 M (Kubota Co., Tokyo, Japan). After the cell debris was removed by centrifugation at 10,000×g at 4 °C for 30 min, the supernatant was obtained as cell-free extract. The enzyme in the cell-free extract was then fractionated by ammonium sulfate precipitation. The precipitant of 20–33% saturation fraction was suspended in 10 mM KPB (pH 8.0) containing 0.1% 2-mercaptoethanol and dialyzed against the same buffer. The dialyzed enzyme solution was applied to a DEAE-Toyopearl column (φ6.0 cm × 13 cm), and the absorbed enzyme was eluted by a linear gradient of 0–0.5 M NaCl. The enzyme solution was next saturated to 20% ammonium sulfate and applied to a Butyl-Toyopearl column (φ3.0 cm × 22.0 cm). A step-wise elution was done with 10 mM KPB buffer containing 20, 10, and 0% of ammonium sulfate saturation. The final preparation gave a single band on SDS-PAGE. Protein concentration was measured using the Bradford method. The specific activity for (R)-**1a** (20 mM) of the purified variants R283G, Y228L/R283G, I230A/R283G, I230C/R283G, and I230F/R283G were calculated to be 2.2, 18.3, 0.58, 0.16, and 0.071 U/mg, respectively. The specific activity toward (R)-phenylalanine (**3**) of the purified wild-type and variant Y228L were shown to be 7.5 and 0.18 U/mg, respectively.

Enzyme Assay

The oxidase activity was assayed at 30 °C by measuring quinoneimine dye formation by determining absorbance at 505 nm with a spectrophotometer. The reaction mixture contained the substrate, 100 mM KPB (pH 8.0), 2 mM phenol, 1.5 mM 4-aminoantipyrine, 2 U horseradish peroxidase, 10% DMSO and varying concentrations of the enzyme. The substrate was dissolved in DMSO. One unit of

enzyme activity was defined as the amount of enzyme that produces 1 µmol of hydrogen peroxide per min.

Kinetic Parameter

The kinetic parameter was determined by the same method as described in the section of the enzyme assay using 1–20 mM (R)-**1a**, 1–5 mM **2a**, and 1–7 mM (RS)-**2c**, (R)-**2c**, and (S)-**2c**. The reaction mixture contained the substrate, 100 mM KPB (pH 8.0), 2 mM phenol, 1.5 mM 4-aminoantipyrine, 2 U horseradish peroxidase, 10% DMSO, and the enzyme at varying concentrations.

The initial velocity was measured spectrophotometrically with the software Spectra Manager Version 2 (JASCO Co., Tokyo, Japan). These experiments were conducted in triplicate. The Michaelis constant (K_m) was determined by using the software KaleidaGraph (Synergy Software, Reading, PA., USA). Catalytic efficiency (k_{cat}/K_m) was calculated by using these results.

Identification of the Product by Enzymatic Deracemization Reaction

The reaction mixture (40 mL) consisted of 100 mM glycine-NaOH buffer (pH 9.0), (RS)-**2c** (50.0 mg, 0.197 mmol), 100 mM NaBH₄, and 4 U purified enzyme was stirred at 1.3 × 10³ rpm at 30 °C for 1 hr in a 1 L eggplant flask. The progress of the reaction was monitored by HPLC with an OD-H column (φ 0.46 cm × 25 cm, Daicel Chiral Technologies Co. Ltd, Tokyo, JAPAN) using a solvent system of hexane: 2-propanol = 9:1 (Absorbance: 220 nm, Flow rate: 1 mL/min, column temperature: 30 °C). The reaction was quenched by addition of 1 M NaOH. The aqueous phase was extracted by hexane (40 mL × 3), and then, the hexane layer was dried *in vacuo*. The remaining product was analyzed by ¹H-NMR and by optical rotation measurement. The ¹H NMR spectra were recorded on the Bruker Biospin AVANCE II 400 (Bruker Biospin, Rheinstetten, Germany) system. Optical rotation was determined by ATAGO AP-300 (Atago Co., Tokyo, Japan) by using a 10.1-mm cell. The optical purity of the isolated (R)-**2c** was 95.7% e.e. with an isolation yield of 46.2% (19.8 mg, 0.091 mmol). The ¹H-NMR spectra were shown as follows: **2c** (400 MHz; DMSO-d₆) δ_H (ppm) 7.18–7.43 (m, 9H), 5.09 (s, 1H), 2.33 (s, 2H). [α]_D²⁷ –9.99° (c 1.0, EtOH) (lit. [α]_D²⁰ –10.6 (c 1.1, EtOH) for the (R)-enantiomer, [α]_D²⁰ +10.8 (c 2.18, EtOH) for the (S)-enantiomer.^[14]

Acknowledgements

This work was supported by a grant from the Exploratory Research for Advanced Technology (ERATO) Asano Active Enzyme Molecule Project from the Japan Science and Technology Agency (JST) (Grant Number JPMJER1102). This research was also supported in part by a grant-in-aid for Scientific Research S from The Japan Society for Promotion of Sciences (No. 17H06169) to Y. Asano. We thank Dr. Kimiyasu Isobe for his critical reading of the manuscript.

Conflict of Interest

The authors declare no conflict of interest.

Keywords: Chiral amine · Amine oxidase · D-amino acid oxidase · Deracemization · Oxidation

- [1] a) D. Ghislieri, N. J. Turner, *Top. Catal.* **2014**, *57*, 284–300; b) J. S. Shin, B. G. Kim, *Enzyme Microb. Technol.* **1999**, *25*, 426–432.
- [2] M. T. Reetz, K. Schimossek, *Chima* **1996**, *50*, 668–669.
- [3] D. Koszelewski et al, *Org. Lett.* **2009**, *11*, 4810–4812.
- [4] a) N. J. Turner, *Nat. Chem. Biol.* **2003**, *5*, 567–573; b) H. Kohls, F. Steffen-Munsberg, M. Höhne, *Curr. Opin. Chem. Biol.* **2014**, *19*, 180–192.
- [5] a) M. J. Abrahamson, E. Vázquez-Figuerosa, N. B. Woodall, J. C. Moore, A. S. Bommarius, *Angew. Chem. Int. Ed.* **2012**, *16*, 3969–3972; b) M. J. Abrahamson, J. W. Wong, A. S. Bommarius, *Adv. Synth. Catal.* **2013**, *17*, 1780–1786.
- [6] a) M. Alexeeva, A. Enright, M. J. Dawson, M. Mahmoudian, N. J. Turner, *Angew. Chem. Int. Ed.* **2002**, *41*, 3177–3180; *Angew. Chem.* **2002**, *114*, 3309–3312; b) D. Ghislieri, A. P. Green, S. C. Willies, I. Rowles, A. Frank, G. Grogan, N. J. Turner, *J. Am. Chem. Soc.* **2013**, *135*, 10863–10869; c) S. Herter, F. Medina, S. Wagschal, C. Benhaim, F. Leipold, N. J. Turner, *Bioorg. Med. Chem.* **2017**, *26*, 1338–1346.
- [7] R. S. Heath, M. Pontini, B. Bechi, N. J. Turner, *ChemCatChem* **2014**, *6*, 996–1002.
- [8] a) K. Yasukawa, S. Nakano, Y. Asano, *Angew. Chem. Int. Ed.* **2014**, *53*, 4428–4431; *Angew. Chem.* **2014**, *126*, 4517–4520; b) N. Kawahara, K. Yasukawa, Y. Asano, *Green Chem.* **2017**, *19*, 418–424.
- [9] S. Nakano, K. Yasukawa, T. Tokiwa, T. Ishikawa, E. Ishitsubo, N. Matsuo, S. Ito, H. Tokiwa, Y. Asano, *J. Phys. Chem. B* **2016**, *120*, 10736–10743.
- [10] a) L. Pollegioni, G. Molla, *Trends Biotechnol.* **2011**, *29*, 276–283; b) A. Caligiuri, P. D'Arrigo, E. Rosini, D. Tessaro, G. Molla, S. Servi, L. Pollegioni, *Adv. Synth. Catal.* **2006**, *348*, 2183–2190; c) L. Pollegioni, S. Sacchi, L. Caldinelli, A. Boselli, M. S. Pilone, L. Piubelli, G. Molla, *Curr. Protein Pept. Sci.* **2007**, *8*, 600–618.
- [11] a) P. F. Fitzpatrick, V. Massey, *J. Biol. Chem.* **1982**, *257*, 12916–12923; b) E. E. Trimmer, U. S. Wanninayake, P. F. Fitzpatrick, *Biochemistry* **2017**, *56*, 2024–2030.
- [12] a) R. S. Heath, M. Pontini, S. Hussain, N. J. Turner, *ChemCatChem*, **2016**, *8*, 117–120; b) V. Köhler, Y. M. Wilson, M. Dürrenberger, D. Ghislieri, E. Churakova, T. Quinto, L. Knörr, D. Häussinger, F. Hollmann, N. J. Turner, T. R. Ward, *Nat. Chem.* **2013**, *5*, 93–99.
- [13] G. A. Aleku, J. Mangas-Sanchez, J. Citoler, S. P. France, S. L. Montgomery, R. S. Heath, M. P. Thompson, N. J. Turner, *ChemCatChem* **2018**, *10*, 515–519.
- [14] T. B. Nguen, Q. Wang, F. Gueritte, *Adv. Synth. Catal.* **2011**, *353*, 257–262.

Manuscript received: April 12, 2018
Accepted Article published: June 23, 2018
Version of record online: July 13, 2018